

## **Performance Study and CFD Predictions of a Ducted Fan System**

Anita I. Abrego  
NASA Ames Research Center  
Moffett Field, CA

I-Chung Chang  
NASA Ames Research Center  
Moffett Field, CA

Robert W. Bulaga  
Millennium Jet Incorporated  
Sunnyvale, CA

AHS Aerodynamics, Acoustics, and Test and Evaluation Technical Specialist Meeting, San Francisco, CA, January 23-25, 2002

### **Introduction**

An experimental investigation was completed in the NASA Ames 7- by 10-Foot Wind Tunnel to study the performance characteristics of a ducted fan. The goal of this effort is to study the effect of ducted fan geometry and utilize Computational Fluid Dynamics (CFD) analysis to provide a baseline for correlation. A 38-inch diameter, 10-inch chord duct with a 5-bladed fixed-pitch fan was tested. Duct performance data were obtained in hover, vertical climb, and forward flight test conditions. This paper will present a description of the test, duct performance results and correlation with CFD predictions.

### **Model Description**

The ducted fan shown in Fig. 1 was mounted on a vertical support as a semispan model in the 7-by 10-Foot Wind Tunnel. Duct angle of attack was achieved by rotating the wind tunnel turntable with a range of 0 to 360 deg. The baseline configuration for this study consisted of a 38-inch diameter, 5-bladed fixed-pitch fan, with a 10-in chord duct and short control vanes. The 4-inch control vanes were located in the duct exit. The vanes had interchangeable 1-inch and 2.25-inch flaps that could be adjusted to  $\pm 40$  deg of deflection, in 10 deg increments. The model was powered by a 125-HP electric motor.

### **Test Conditions**

The ducted fan was tested in both axial flow conditions, representing hover and vertical flight, and cross-flow conditions, representing cruise (Fig.2). The large size of the model relative to the test section meant that the model generated significant flow through the tunnel even when the tunnel drive was off. The model was run at  $\pm 90$  deg angle of attack to create different axial flow conditions. At these conditions, the wind tunnel was run at low speeds against the flow generated by the model to achieve near-zero and even negative inflows. For cruise conditions, the model angle of attack was varied between +5 deg and -25 deg. Control effectiveness of the flapped vanes was tested in both axial and cross flow conditions. The maximum tunnel speed was approximately 135 fps (92 mph); the maximum fan speed was approximately 3400 rpm (560 fps tip speed).

Forces and moments on the ducted fan were acquired from the wind tunnel scale system. Motor torque was measured with an instrumented support arm. The duct, fan hub centerbody, and one fan blade were tufted for flow visualization.

As a result of model induced flow in the wind tunnel, axial flow data points clustered in two advance ratio regions,  $J = 0.05 - 0.10$  and  $J = 0.20 - 0.25$ . The lower range occurred when the ducted fan blows opposite to the normal flow direction of the wind tunnel (larger tunnel losses); the higher range was the result of directing the fan flow along the normal tunnel direction. Lower advance ratios were achieved by using the wind tunnel system to blow against the ducted fan induced flow. Points near hover,  $J = 0$ , were achieved. Baseline performance data will be presented for the axial flow condition (Fig 3-4). Axial flow represents hover, vertical climb, and vertical descent. The effects of forward flight, flap deflection, and geometry changes will also be discussed.

### CFD Prediction

An axisymmetric Navier-Stokes solver was employed to calculate the flow field of a ducted fan (Ref.3). The effects of the spinning rotor blades were introduced to the flow field as sources in the momentum equations. These source terms were not known a priori but are the result of the flow solution at the end of each iteration step. This approach provided a very rapid solution procedure for complicated flow problems.

Preliminary CFD predictions of duct performance are shown in Fig. 5. The flow field of the ducted fan, at 4500 rpm, is also shown in Fig. 6. Further correlation between test data and CFD predictions will be presented in the full paper.

### References

1. Mort, K.W., "Performance Characteristics of a 4-Foot-Diameter Ducted Fan at Zero Angle of Attack for Several Fan Blade Angles," NASA TN D-3122, December 1965.
2. Mort, K.W. and Gamse, B., "A Wind Tunnel Investigation of a 7-Foot-Diameter ducted Propeller," NASA TN D-4142, August 1967.
3. Rajagopalan, R. G. and Zhang, Z., "Performance and Flow Field of a Ducted Propeller," AIAA-89-2673, July 1989.
4. Black, D.M. and Wainauski, H.S., "Shrouded Propellers - A Comprehensive Performance Study," AIAA 5<sup>th</sup> Annual Meeting and Technical Display, Philadelphia, PA, Oct 1968.
5. Ham, N.D. and Moser, H.H., "Preliminary Investigation of a Ducted Fan in Lifting Flight," Journal of the American Helicopter Society, Vol. 3, No. 3, July 1958.
6. Yaggy, P.F. and Goodson, K.W., "Aerodynamics of a Tilting Ducted Fan Configuration," NASA TN D-785, March 1961.
7. Goodson, K.W. and Grunwald, K.J., "Aerodynamic Characteristics of a Powered Semispan Tilting-Shrouded-Propeller VTOL Model in Hovering and Transition Flight," NASA TN D-981, January 1962.

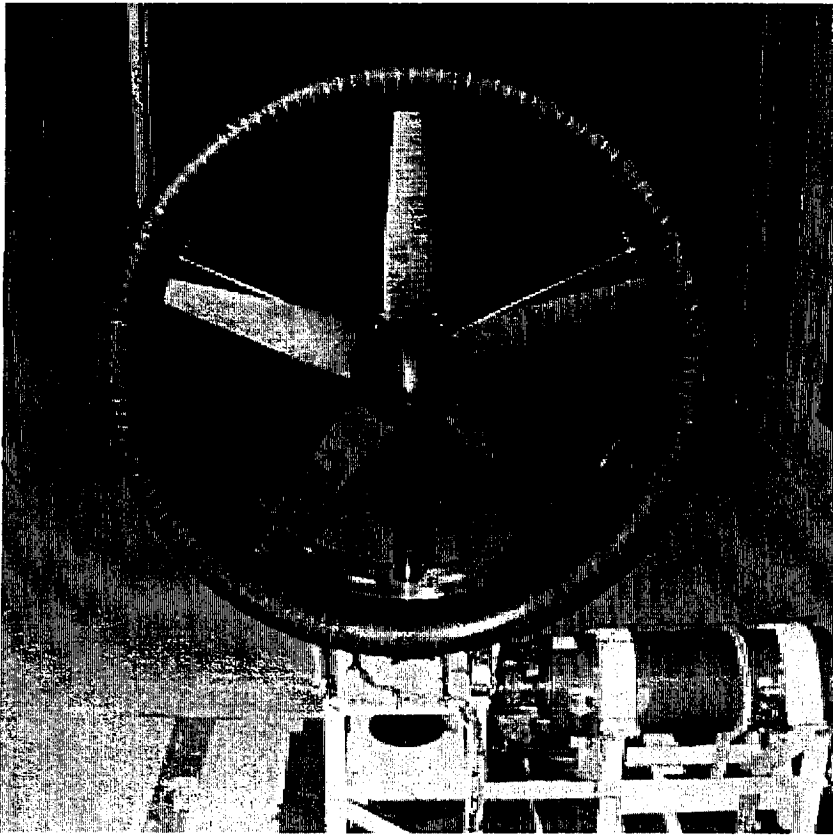


Figure 1. Ducted fan in the Army/NASA 7- by 10-Foot Wind Tunnel.

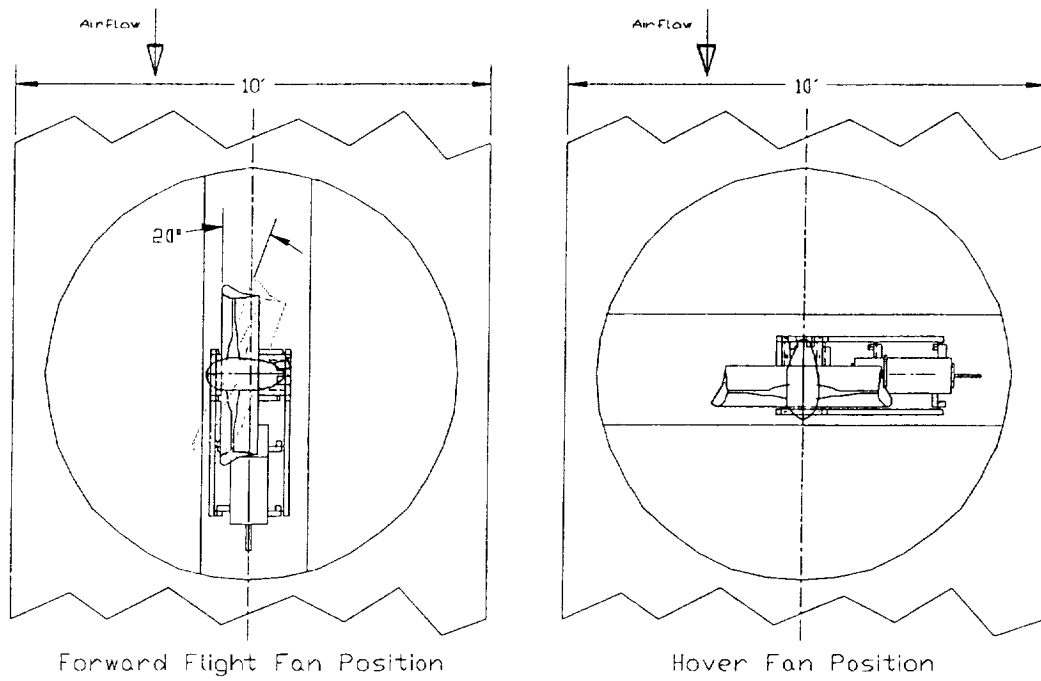


Figure 2. Ducted fan test configuration.

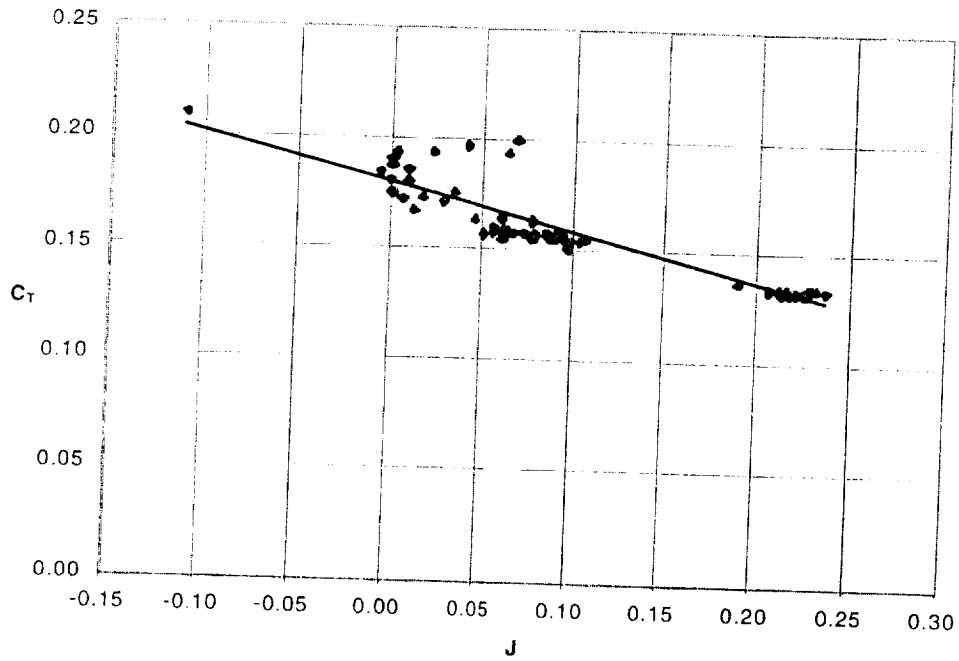


Figure 3. Thrust coefficient as a function of advance ratio for the baseline configuration in axial flow.

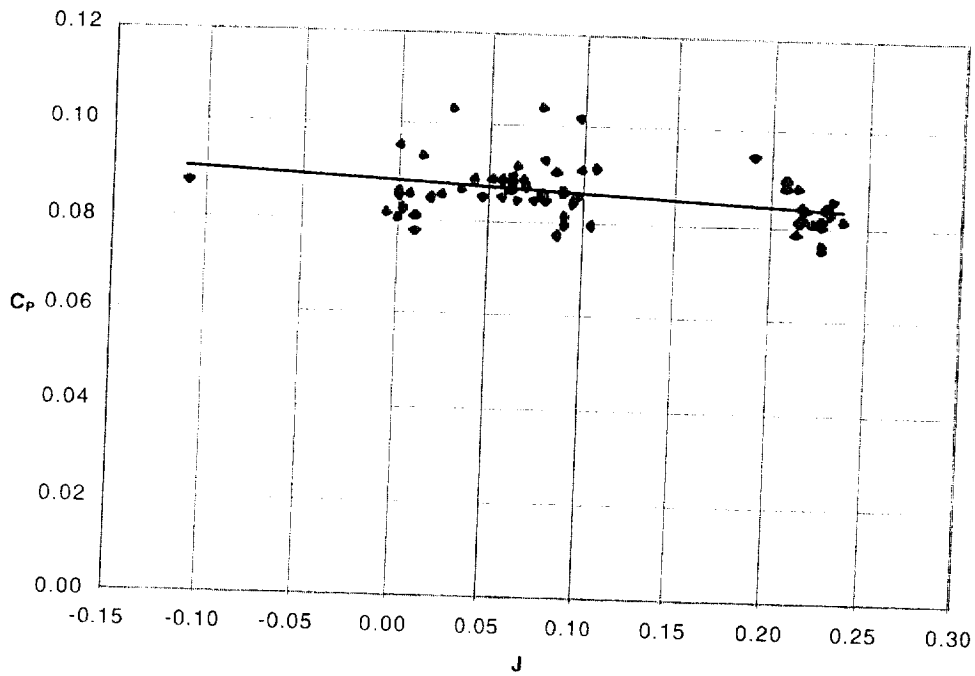


Figure 4. Power coefficient as a function of advance ratio for the baseline configuration in axial flow.

## Torque and Thrust Predictions

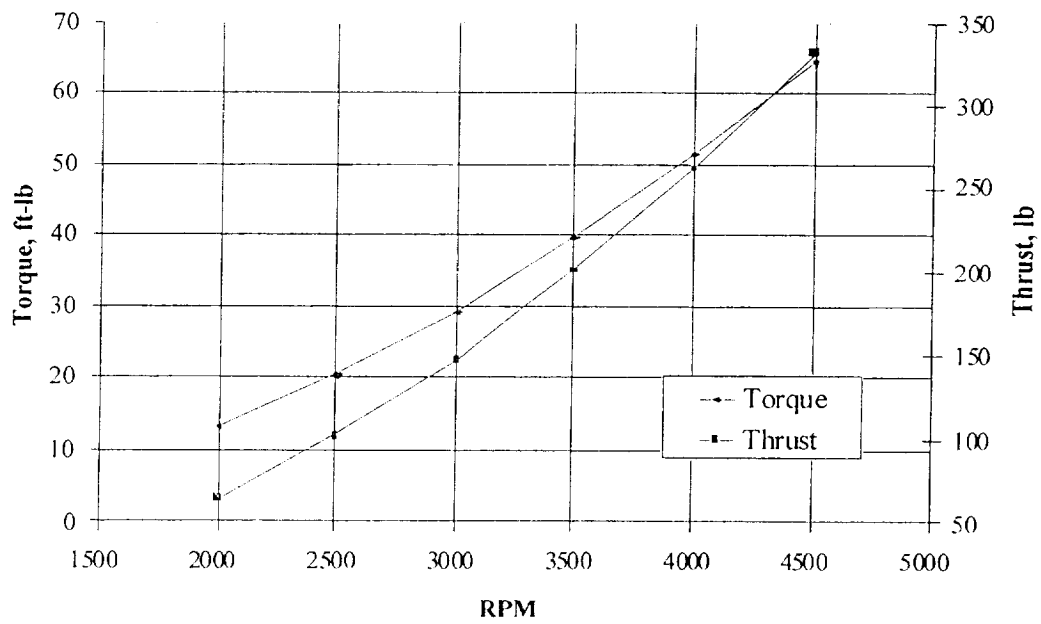


Figure 5. Preliminary CFD predictions of duct performance.

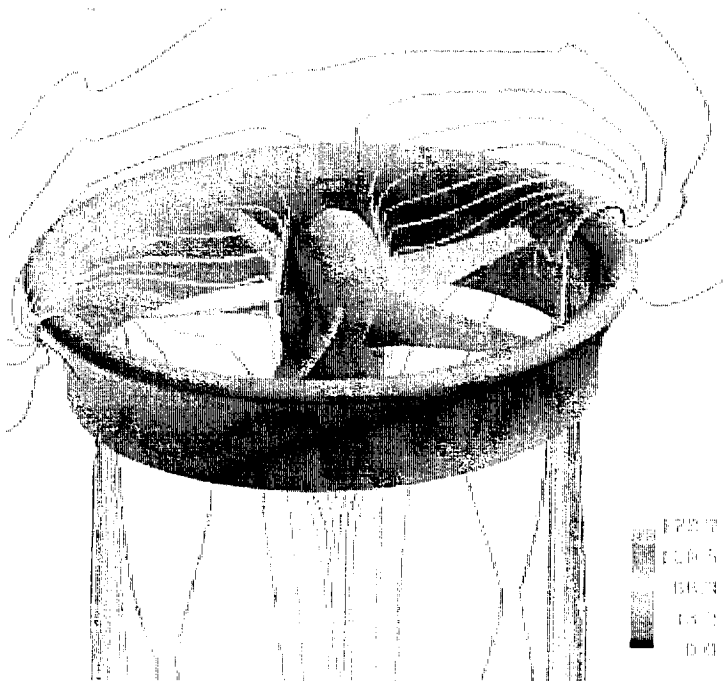


Figure 6. Velocity contours of ducted fan at 4500 rpm.

